Published in final edited form as:
Langmuir. 2012 April 17; 28(15): 6348–6355. doi:10.1021/la300482x.

Homogeneity, Modulus and Viscoelasticity of Polyelectrolyte Multilayers by Nano-Indentation: Refining the Buildup Mechanism

Ali M. Lehaf, **Haifa H. Hariri**, and **Joseph B. Schlenoff***
Department of Chemistry and Biochemistry, The Florida State University, Tallahassee, Florida 32306

Abstract

Atomic force microscopy, AFM, and nanoindentation of polyelectrolyte multilayers, PEMUs, made from poly(diallyldimethylammonium), PDADMA, and poly(styrene sulfonate), PSS, provided new insight into their surface morphology and growth mechanism. A strong odd/even alternation of surface modulus revealed greater extrinsic (counterion-balanced) charge compensation for fully hydrated multilayers ending in the polycation, PDADMA. These swings in modulus indicate a much more asymmetric layer-by-layer growth mechanism than previously proposed. Viscoelastic properties of the PEMU, which may contribute to cell response, were highlighted by variable indentation rates and minimized by extrapolating to zero indentation rate, at which point the surface and bulk equilibrium moduli were comparable. Variations in surface composition were probed at high resolution using force mapping and the surface was found to be uniform, with no evidence of phase separation. AFM comparison of wet and dry films terminated with PSS and PDADMA revealed much greater swelling of the PDADMA-terminated PEMU by water, with collapse of surface roughness features in dry conditions. Dynamic and static contact angle measurements suggested less rearrangement for the glassy PSS surface.

Introduction

There has been much recent interest in the mechanical properties of ultrathin films of polyelectrolyte complex made by the layer-by-layer method.[1–8] These polyelectrolyte multilayers, PEMUs,[9] are hydrated blends of oppositely charged polymers held together by a dense network of ion pair crosslinks.[4,10–12] Their modulus, analyzed using classical approaches to rubber elasticity, is controlled by the internal crosslink density, which is, in turn, regulated by external stimuli such as salt concentration,[4,13–14] pH[2] or redox potential.[15] An important niche for the use of PEMUs is at the interface between cells and synthetic surfaces. PEMUs regulate the adsorption of protein, including those critical for cell adhesion,[16–21] and their mechanical properties have been used to promote adhesion, phenotype and even differentiation (of stem cells).[2,6–7,22–24]

The various techniques used to assess the mechanical properties of PEMUs include the quartz crystal microbalance (QCM),[13,25–26] osmotic swelling,[27–28] and strain-induced buckling.[29] Jaber et al. studied the mechanical properties of sufficiently thick multilayers by

Corresponding Author: schlen@chem.fsu.edu.

Supporting Information
Layer-by-layer buildup of PDADMA/PSS multilayers showing the difference between the wet and dry thickness. Difference in dry modulus for PDADMA and PSS ending films, table of wet thickness and modulus measurements at different number of layers, sample force curve fitted to punch model, surface contour of dry and wet PDADMA and PSS ending films, mechanical homogeneity of dry PSS and PDADMA ending films. This material is available free of charge via the Internet at http://pubs.acs.org.

tensile stress relaxation.[4] Nanoindentation remains the most widely employed method to study the elasticity of ultrathin films.[2,6–8,22,30] Because of experimental challenges of making measurements on ultrathin films, most of these approaches have focused on the elastic components of the modulus,[7,26–27,29] obtained at sufficiently long times, or slow rates, to allow viscous components to decay. Despite the extensive use of nanoindentation, the viscosity response is often ignored in the measurement of an "apparent" modulus.[2,6–8,22] Given the recently-demonstrated role of the viscous (loss) modulus of substrate thin films in determining the fate of adherent cells,[31] time, or rate, of deformation is a highly relevant parameter.

Nanoindentation also provides insight into the mechanism of PEMU buildup. For example, in a recent study of photocrosslinking in weak acid PEMUs, we showed that the apparent modulus is a strong function of the identity of the last-added or "top" layer of polyelectrolyte.[8] Such a fluctuation in modulus is one example of the odd/even oscillations in PEMU properties found extensively in the field: in addition to the expected switching of surface charge between positive and negative layers,[32–33] the contact angle,[34–35] interpreted to reveal "hydrophobicity," depends on the terminating layer.[19,36] Odd/even effects were also observed in the mobility of water in multilayers measured by NMR relaxation rates.[37–38] The adsorption of PAH on the surface decreased the water mobility for PAH/PSS systems.[38–40]

In the present work we use nanoindentation to reveal some important fundamental properties of PEMUs made from poly(diallyldimethylammonium chloride), PDAMDAC, and poly(styrene sulfonate), PSS. The results are compared with the extensive knowledge base of PEMUs from these two components which enables conclusions on both their surface morphology and their buildup mechanism.

Materials and Methods

Poly(4-styrenesulfonic acid) ($M_w = 7.5\times10^4$ g mol^{-1}) and poly(diallyldimethylammonium chloride) ($M_w = 40\times10^4 - 50\times10^4$ g mol^{-1}) were used as received from Aldrich. NaCl (ACS grade) from Aldrich was used to adjust the ionic strength of the polyelectrolyte solutions and for the doping solutions. All solutions were prepared using deionized water (Barnstead, 18 MΩ E-pure).

Polyelectrolyte multilayer buildup

Multilayers made from PDADMA and PSS were built with the aid of a robot (StratoSequence V, nanoStrata Inc.) on silicon wafer substrates that were cleaned with "piranha" reagent (70% H_2SO_4 and 30% H_2O_2. Caution: piranha is a strong oxidizer and should not be stored in closed containers), rinsed vigorously with distilled water followed by drying with a flow of N_2. Polyelectrolyte solutions were 10 mM based on the monomer repeat unit, and the ionic strength was fixed using NaCl at 1.0 M. The substrates were mounted on a shaft that rotated at 300 rpm. The dipping time in the polymer solutions was 5 min followed by three 1 min rinsing steps in water after each layer. $(A/B)_x$ and $(A/B)_xA$ indicate a multilayer ending in B and A respectively, where x is the number of layer pairs, A represents the polycation and B the polyanion.

A Gaertner Scientific L116S autogain variable angle Stokes ellipsometer was used to obtain the dry thickness of PEMU films unless stated otherwise. Ten thickness measurements on each PEMU were averaged. A KSV Cam 200 was used to determine the static contact angle of the PEMU films. The volume of water droplet was 10 μl for all measurements and each point was an average of 3 measurements taken at different spots on the PEMU. Dynamic contact angles, DCAs, (both advancing Θ_a and receding Θ_r) were recorded using the

Wilhelmey plate technique (Cahn Instruments, DCA 300). For DCA, the immersion rate of the PEMU, built on a double-side-polished Si wafer, in water was 100 μm sec^{-1}.

Force spectroscopy

The stiffness of the films, represented by the apparent modulus, was determined by force-indentation measurements, or force curves, using an atomic force microscope (AFM). An MFP-3D AFM unit was equipped with an ARC2 controller (Asylum Research Inc., Santa Barbara, CA) and Igor Pro software. AC240-TS tips were used, with spring constant ~ 2 N m^{-1}. The optical lever sensitivity (OLP) of the tip was first calibrated in air and then its spring constant was determined by the thermal fluctuation technique. The sample was then immersed in salt solution at a given concentration and the OLP of the tip was recalibrated. Force maps of 4 × 5 points were performed on the PEMU *in situ* with a scan size of 20 × 20 μm. The distance from the surface and the velocity of the tip were set to 500 nm and 1μm s^{-1} respectively unless stated otherwise. The term “apparent” modulus is used to describe the modulus recorded at a specific tip velocity. For viscoelasticity studies, force curves were performed at indentation velocities ranging from 50 nm/sec to 3.17 μm/sec on the PDADMA/PSS multilayer.

The applied force and the resulting indentation are given by

$$F_{applied}=Kd=K(z-\delta) \tag{1}$$

$$\delta=(z-d) \tag{2}$$

where δ is the indentation of the tip into the material, here, typically up to about 50 nm, z is the distance of the tip relative to the material in the z-direction, d is the deflection of the tip, and K is the spring constant of the cantilever. All force curves were analyzed using Hertzian contact mechanics for a punch model as in Equation 3.

$$F_{punch}=2E_c R(z-d) \tag{3}$$

E_c is the convoluted modulus of the material and R is the radius of the indenter. Equation 3 predicts force is proportional to indentation, which was the case observed here, as shown in the sample force curve in Supporting Information

By fitting the force *vs*. indentation curves, E_c, can be obtained and related to the apparent modulus E_1 of the indented material and E_2 (of the indenter) using Equation 4. The radius of the AC240-TS tip was 10 nm as provided by the manufacturer

$$E_c=\left(\frac{1-\upsilon_1{}^2}{E_1}+\frac{1-\upsilon_2{}^2}{E_2}\right)^{-1} \tag{4}$$

In Equation 4, υ_1 and υ_2 are the Poisson ratios of the multilayer and the silicon indenter. υ_2 was fixed at 0.27, E_2 was set to 150 GPa. υ_1 was assumed to be 0.5 as the PEMUs were considered to be isotropic elastic materials in the range of loads applied.

Imaging

Wet and dry images of the surface of PEMUs were recorded under AC and contact mode to obtain the morphology, surface roughness and thickness of the films. AC240-TS tips were

used for dry and wet imaging of PSS-ending multilayers. A softer tip, TR400PSA (spring constant ~0.02 N m^{-1} and 20 nm radius) was required for PDADMA-ending films in liquid. The cantilever was tuned to resonate below its resonance frequency by 10%. The scan size was 5 × 5 μm or 10 × 10 μm and scan rate was 0.5Hz. Wet and dry thickness was measured by scanning over a scratch step edge. The rms roughness of the image was obtained on a 1 × 1 μm patch. Ten roughness values were averaged for each data point.

Results and Discussion

Swelling and mechanical properties

Recently, we showed that a hydrated PEMU surface ending in poly(acrylic acid) (PAA) was stiffer than a PEMU ending in poly(allylamine hydrochloride) (PAH).[8] This result was somewhat surprising, since we expected a PAA layer to be more hydrophilic and softer. In the present work, stiffness as a function of the identity of the terminating layer was investigated for a different set of polyelectrolytes, both having pH-independent charges.

PDADMA/PSS multilayers built from 1.0M NaCl were evaluated by nanoindentation starting with a 14-layer film, which was thick enough (about 500 nm wet) to measure a PEMU modulus independent of the substrate (at least 150 nm of thickness is required for our experimental setup). Buildup continued from 1.0 M NaCl and measurements were made on the following layer numbers: 15, 18, 19, 22, 23, 26, 27, 30, 31, 40, 41, 50 and 51. After each layer the multilayer was rinsed in water, dried under a flow of nitrogen then dipped in 10 mM NaCl for 12 h. The salt concentration was maintained at a low value to provide a defined ionic strength yet avoid annealing of the surface features and doping which occurs over time at high [NaCl].[10] Thickness, taken by scanning the AFM tip over the scratch, and force curve measurements were performed *in situ* in 10 mM NaCl. Figure 1 shows the variation of apparent Young's modulus and wet thickness as a function layer number. For layer numbers higher than 15 (wet thickness of 527 nm) the apparent modulus of either PSS- or PDADMA-terminated films remained roughly constant but there was a large consistent difference between the two. The PSS-ending layer had an average modulus of about 80 MPa, while that for the multilayer ending in PDADMA had an average modulus of about 11 MPa. This trend correlated well with the change in wet thickness: when PDADMA was added the multilayer was more swollen i.e. more hydrated, in contrast to the addition of a PSS layer, which maintained or slightly decreased the thickness (see Figure 1).

The dramatic difference in modulus and hydration between layers was only observed with PEMUs exposed to solution. Dried multilayers did not show these swings in modulus and thickness (see Supporting Information Figure S1 and S4). Our data is entirely consistent with odd-even alternations in PEMU hydration observed with other techniques. For example, Miller et al. used ellipsometry to study the swelling of different PEMUs as a function of the end layer, ionic strength, and the swelling solvent. They found that PDADMA-ending films swelled in water more than PSS ending ones.[41] Ramos *et al*., using a combined ellipsometer and quartz crystal microbalance, found that PDADMA-terminated multilayers had a higher water content, and were softer, than PSS- terminated ones.[42] In contrast, for a PAH/PSS multilayer, Wong *et al*.[36] found PSS-ending multilayers were more swollen than those terminated in PAH. Smith *et al*.,[37] and McCormick *et al*.,[38] using ^{13}C and ^{1}H NMR, found that the mobility of PSS remains constant during PEMU buildup while that of PDADMA decreases. Also, by ^{1}H NMR they showed water was more mobile and there was a chemical shift when the PEMU was capped with PDADMA. Using ATR-FTIR we showed that the hydration differences were localized to the surface of the multilayer (about the top 10 layers), which is rich in extrinsic charge. Oscillations in hydration were not seen in the interior of the PEMU.[43]

Modulus versus doping by salt

Stoichiometric polyelectrolyte multilayers, and complexes in general, swell when immersed in solution of reasonably high salt concentration. This expansion, an example of "antipolyelectrolyte" behavior, is due to doping by salt ions, which almost always bring an excess of water into the complex with them. A certain decrease in modulus is expected from the volume expansion and additional hydration, but the modulus actually decreases substantially, which is due to the breaking of ion pair crosslinks within the material.

When polyelectrolyte charges are not matched 1:1 a significant counterion population exists within the complex, even when it is immersed in water. These extrinsic charged sites exert osmotic pressure, swelling the complex. On the addition of salt the complex dehydrates due to the external osmotic pressure and the material shrinks (the "polyelectrolyte" effect). With enough external salt, the expansion due to doping overwhelms the shrinkage due to osmotic dehydration of extrinsic sites. Thus, early AFM measurements on the swelling of multilayers revealed a minimum in the thickness versus [NaCl] data.[10] It was also shown that much of the residual counterion content could be "annealed" out by exposure to high [NaCl], which promotes chain mobility.[10]

Although modulus is known to decrease with doping,[4,13] nanoindentation *vs*. salt doping has not previously been reported. Figure 2 depicts the apparent *in situ* modulus *vs.* [NaCl] for a PDADMA/PSS PEMU. The data shows a shallow peak in modulus on increasing salt concentration for an as-made PEMU. When the salt concentration subsequently decreases this feature is missing. The behavior may be reconciled by comparison with the previously published thickness *vs*. [NaCl] data, which shows a clear minimum in thickness *vs*. [NaCl] at about 0.25M, due to the osmotic dehydration described above.[10,43] After the PEMU reaches 1.5M NaCl it is annealed and exhibits "antipolyelectrolyte" behavior only on decreasing [NaCl].

The apparent modulus values in Figure 2 are much higher than those reported by Jaber et al. [4] at corresponding [NaCl]. As shown later, this is because the latter were collected by stress relaxation after the viscous components of the viscoelasticity were allowed to decay.

Nano-viscoelastic nature of PEMUs

As shown by tensile measurements on microcoupons of PDADMA/PSS,[14] the viscoelastic properties of multilayers lead to time/frequency dependent mechanical properties. At sufficiently low frequency, or long times, the viscous components of the material disappear to leave only the "equilibrium" elastic modulus. The time-dependent parameter for nanoindentation is the indentation rate. Here, force curve measurements were performed on un-annealed $(PDADMA/PSS)_{15}$ (PSS ending) multilayer, and on the same multilayer that was annealed in 1 M NaCl for 5 days, at different indentation velocities, which are equivalent to different strain rates. All force curve measurements were done in 10 mM NaCl. A plot of apparent Young's modulus *vs*. indentation velocity, shown in Figure 3, reveals a significant increase in apparent modulus with increasing indentation rate. Extrapolating to zero strain rate gives a modulus of about 15 MPa, the "equilibrium" elastic modulus, roughly the same as obtained previously for PDADMA/PSS microcoupons.[4] No difference was found in the apparent modulus at different indentation velocities between the annealed and the un-annealed multilayer. This finding that the PSS-ending surface PEMU layer has similar mechanical properties to bulk, stoichiometric PEMU leads to the conclusion that its composition is also similar (i.e. it is close to stoichiometric PDADMA:PSS).

The viscous response of PEMUs is rarely considered in nanoindentation measurements. Using the deformation of capsules by AFM probes, Mueller *et al*. observed elastic response

for multilayers below about 35 °C and a rate dependent viscoelastic response above this temperature.[44] Using a spherical indenter and a thick PEMU, Francius *et al*. recorded deflections as a function of approach velocity over three orders of magnitude and were able to extract a roughly constant elastic modulus over this range of velocities.[45] Lu *et al*. characterized the linear viscoelastic behavior of single wall carbon nanotube/polyelectrolyte multilayers using nanoindentation where the viscoelastic function was measured using one of two methods: (1) direct differentiation from the load-displacement data and (2) by fitting the analytical load-displacement relation to the nanoindentation data known as the material parameter extraction method.[46] The viscous component of PEMU mechanical response probably has an important contribution to the behavior of cells grown on them. For example, Cameron *et al*. prepared a series of polyacrylamide gels with the same storage modulus but different loss modulus.[31] It was found that by increasing the loss modulus, the spread and proliferation of human mesenchymal stem cells increased and the size and maturity of focal adhesions decreased. Also, the change in loss modulus had an impact on the differentiation of these cells with more differentiation on the substrates with higher loss modulus.[31] Mehrotra *et al*. recently analyzed cell adhesive behavior in terms of an attempt by cells to achieve homeostasis of adhesion energy.[24] If a viscous component comes into play, homeostasis may be achieved by balancing adhesion power (energy per unit time). In other words, the damping efficiency of the PEMU may be an important parameter.

Surface roughness is not due to phase separation

It is well known that the surface roughness of multilayers generally increases with film thickness.[25,47–50] There are exceptions to this, notably some exponentially grown systems, which may be fluid enough for the surface to relax and minimize the interfacial contact area.[51] Alternatively, sufficient salt added to a system promotes enough polyelectrolyte interdiffusion to smooth the surface.[10] The source of the roughness has long puzzled those in the field. It has the appearance of a surface-induced phase separation (spinodal decomposition) between the two polyelectrolytes, and this mechanism was, indeed, recently put forward.[52]

Phase separations are not uncommon in PEMUs. Mendelsohn *et al*. described the formation of micropores in PAH/PAA PEMUs. The pores, which appeared as a result of a pH change, were attributed to spinodal decomposition on protonation of carboxylic acid allowing reorganization and phase separation from the acidic water solvent.[53] Fery *et al*., describing the formation of nanopores in PAH/PAA PEMUs prepared from salt solution and immersed in pure water, presented pore formation as a dewetting mechanism rather then spinodal decomposition.[54]

As seen in Figure 1, surface modulus in the fully hydrated state is a strong function of composition. Thus, any lateral variation in surface composition should manifest by a variation in surface modulus. To map the surface modulus of a PEMU, a $(PDADMA/PSS)_{16}$ multilayer was built from 1.0 M NaCl. Using the AC240TS tip, a contact mode AFM image was taken of the multilayer *in situ* immersed in 10 mM NaCl. The image, shown in Figure 4, had a surface roughness of 70 nm. Various points on the PEMU corresponding to “hills” and “valleys” were selected (14 of each) for force curve measurements. Their locations are shown on Figure 4. The average modulus on the hills (47±4 MPa) was the same as in the valleys (49±4 MPa) within experimental error. In other words, although the multilayer is quite rough, the surface composition is uniform and there is no evidence of phase separation.

Figure 4 provides additional points of interest. It shows a to-scale representation of the surface features and the AC240T tip, with a cone angle of 35°. Only the first μm of the 14 μm tip length is shown here. The 20 nm diameter tip is easily small enough to interrogate the features of the multilayer surface. Also, the surface and z-axis have been replotted so they

are equal. Usually, AFM micrographs present a much finer z-axis than horizontal axis, causing the surface to appear more mountainous than it really is. In other words, the surface undulates over quite a long length scale, far greater than the dimensions of a molecule.

Implications for the mechanism of multilayer buildup

The observations above provide significant insight into the way polyelectrolyte adds to the growing multilayer. When a PDADMA "layer" adsorbs, the surface is much softer than when PSS adsorbs. Further, a PSS-terminated surface has similar mechanical properties to a bulk, stoichiometric PDADMA/PSS PEMU. It has been shown that polyelectrolyte complex is softer when compensated extrinsically rather than intrinsically.[4] Intrinsic compensation yields maximally crosslinked (via ion pairs), minimally hydrated complex. Softening is a signature of extrinsic compensation (counterion content). Thus, it can be concluded that a PDADMA-terminated surface is significantly extrinsic whereas one terminated by PSS is highly intrinsic. The comparison is illustrated in Scheme 1, which shows excess polymer charge, and counterions throughout the surface of a PDADMA-capped PEMU, and an almost intrinsic surface when PSS is adsorbed. If this were the case, one might expect incomplete surface charge reversal is possible with a PSS layer, which has, in fact, been observed for PDADMA/PSS PEMUs under some conditions.[33]

Previous models of multilayer growth have assumed equal overcompensation for both polyelectrolytes.[9,55] If the PSS merely compensates the existing PDADMA at the surface it is the latter that controls the rate of multilayer growth. The "asymmetric" growth mode described here for the linearly-growing PDADMA/PSS PEMU is reminiscent of the mechanism for exponential growth of some systems, where at least one of the components is able to access the entire film.

The effects of asymmetric growth and the excess of extrinsic charge for the PDADMA-terminated films are best seen by comparing wet *versus* dry PEMUs. Figure 5A depicts AFM images of a dry PSS-terminated 30-layer film and the same film imaged *in situ* while immersed in 10 mM NaCl. Some swelling of the surface features is observed but the overall roughness does not change much (rms roughness was 66 nm and 70 nm for dry and wet PEMU, respectively). For comparison, the dry 31-layer PDADMA-terminated multilayer, Figure 5B, is *smoother* than its PSS predecessor. Also in contrast, the immersed PDADMA-topped film, which was quite difficult to image (being much softer, see Figure 1), is highly swollen and much rougher (rms roughness was 16 nm for the dry PEMU and 106 nm for the wet). The differences in behavior and morphology are consistent with Scheme 1, where the highly-intrinsic PSS surface swells only slightly whereas the PDADMA surface is much more extrinsically compensated, and therefore hydrated. The PDADMA surface has so much extrinsic charge it resembles a brush- or mushroom-like polyelectrolyte conformation (although the lateral features are much larger than a single chain).

Contact angle measurements

The oscillation of water contact angle values on PEMUs, depending on the top layer, was one of the earliest reported odd-even phenomena.[34–35] It has been assumed that one of the polyelectrolytes is more "hydrophobic," and the multilayer buildup properties may be rationalized with such a classification. In fact, contact angle measurements are rarely made under equilibrium conditions.[56] To illustrate this, dynamic advancing and receding contact angle measurements, using the Wilhelmy plate technique, were made on the PDADMA/PSS multilayer. These were complemented with a "static" contact angle, which measures the angle made at the surface/liquid/air interface by a sessile drop.

Figure 6 shows oscillations of the static contact angle with the identity of the last layer, as usually observed in multilayers.[34–35] Surface roughness on the length scale of these PEMUs can increase contact angles on hydrophobic surfaces and decrease them on hydrophilic ones.[57] These large swings in angle might lead one to believe there are pronounced differences in hydrophobicity between polyelectrolytes. However, the trend of the contact angle data, suggesting PSS is more hydrophilic than PDADMA, appears to be at odds with the swelling data above showing the PDADMA-terminated layer to be more hydrated. The non-equilibrium, or history-dependent, nature of the contact angle measured here is revealed by a comparison of the dynamic advancing, Θ_a, *versus* receding, Θ_r, angle. Whereas Θ_a and Θ_r are close for the PSS terminated surface, they diverge strongly for PDADMA termination. This difference is consistent with minor surface rearrangement of the more glassy PSS-capped PEMU. The PDADMA surface, on the other hand, undergoes strong volume transitions and what looks like a collapsed layer on emersion and drying (Figure 5B). It is not surprising that the contact angle depends on history for the latter system (i.e. whether it is being immersed/wetted, or emersed/dried).

PEMUs are used to enhance surface wettability, especially on rough surfaces, as recently described for microtextured titanium implants.[58] Figure 6 suggests wetting of a dry multilayer-covered surface is not a simple matter of selecting the surface that provides the most hydrated polymer (logic which would lead to the wrong choice here). The glassy, immobile nature of the PSS-terminated PEMU surface likely maintains the charged, hydrophilic sulfonate group (compensated by sodium, a well-hydrated cation) near the polymer/air interface when the multilayer dries. For comparison, PAH/PAA multilayers terminated in PAA, also glassy and Na^+ compensated,[8] provide even lower static contact angles.[35]

Conclusions

Straightforward AFM measurements have cast light on several aspects of PDADMA/PSS multilayers. First, the surface modulus of fully hydrated films (immersed in solution) oscillates significantly during buildup, with PDADMA-terminated PEMUs having a softer surface. These oscillations (and the deductions made) are not observed with dried PEMUs. Alternations in water content, seen here and previously, are consistent with greater extrinsic compensation for PDADMA-terminated films. In fact, the PSS-terminated samples show little sign of extrinsic compensation, as their modulus is about the same as that of bulk (intrinsic) PEMU. The differences in level of extrinsic compensation are at odds with previous mechanisms for layer-by-layer buildup of polyelectrolytes, where it was assumed that each layer overcompensates the surface charge by the same amount. Although the surface of PEMUs was rough and appeared to be phase separated, as is typical for many types of multilayers, surface mapping using the dependence of modulus on composition provided evidence to the contrary. The soft, extrinsic, brush-like properties of PDADMA-ending PEMUs explains why they are so good at “sponging” up negative proteins like serum albumin.[59]

Supplementary Material

Refer to Web version on PubMed Central for supplementary material.

Acknowledgments

This work was supported by grants from the National Institutes of Health (R01EB006158) and the National Science Foundation (DMR-0939850).

References

1. Mermut O, Lefebvre J, Gray DG, Barrett CJ. Structural and Mechanical Properties of Polyelectrolyte Multilayer Films Studied by AFM. Macromolecules. 2003; 36:8819–8824.
2. Thompson MT, Berg MC, Tobias IS, Rubner MF, Van Vliet KJ. Tuning Compliance of Nanoscale Polyelectrolyte Multilayers to Modulate Cell Adhesion. Biomaterials. 2005; 26:6836–6845. [PubMed: 15972236]
3. Schneider A, Francius G, Obeid R, Schwinté P, Hemmerlé J, Frisch B, Schaaf P, Voegel JC, Senger B, Picart C. Polyelectrolyte Multilayers with a Tunable Young's Modulus: Influence of Film Stiffness on Cell Adhesion. Langmuir. 2006; 22:1193–1200. [PubMed: 16430283]
4. Jaber JA, Schlenoff JB. Mechanical Properties of Reversibly Cross-Linked Ultrathin Polyelectrolyte Complexes. J Am Chem Soc. 2006; 128:2940–2947. [PubMed: 16506773]
5. Picart C, Senger B, Sengupta K, Dubreuil F, Fery A. Measuring Mechanical Properties of Polyelectrolyte Multilayer Thin Films: Novel Methods Based on AFM and Optical Techniques. Colloids Surf, A. 2007; 303:30–36.
6. Pozos Vázquez C, Boudou T, Dulong V, Nicolas C, Picart C, Glinel K. Variation of Polyelectrolyte Film Stiffness by Photo-Cross-Linking: A New Way To Control Cell Adhesion. Langmuir. 2009; 25:3556–3563. [PubMed: 19275180]
7. Moussallem MD, Olenych SG, Scott SL, Keller TCS, Schlenoff JB. Smooth Muscle Cell Phenotype Modulation and Contraction on Native and Cross-Linked Polyelectrolyte Multilayers. Biomacromolecules. 2009; 10:3062–3068. [PubMed: 19817347]
8. Lehaf AM, Moussallem MD, Schlenoff JB. Correlating the Compliance and Permeability of Photo-cross-linked Polyelectrolyte Multilayers. Langmuir. 2011; 27:4756–4763. [PubMed: 21443175]
9. Decher G. Fuzzy Nanoassemblies: Toward Layered Polymeric Multicomposites. Science. 1997; 277:1232–1237.
10. Dubas ST, Schlenoff JB. Swelling and Smoothing of Polyelectrolyte Multilayers by Salt. Langmuir. 2001; 17:7725–7727.
11. Farhat TR, Schlenoff JB. Ion Transport and Equilibria in Polyelectrolyte Multilayers. Langmuir. 2001; 17:1184–1192.
12. Farhat TR, Schlenoff JB. Doping-Controlled Ion Diffusion in Polyelectrolyte Multilayers: Mass Transport in Reluctant Exchangers. J Am Chem Soc. 2003; 125:4627–4636. [PubMed: 12683835]
13. Salomäki M, Laiho T, Kankare J. Counteranion-Controlled Properties of Polyelectrolyte Multilayers. Macromolecules. 2004; 37:9585–9590.
14. Jaber JA, Schlenoff JB. Dynamic Viscoelasticity in Polyelectrolyte Multilayers: Nanodamping. Chem Mater. 2006; 18:5768–5773.
15. Reisch A, Moussallem MD, Schlenoff JB. Electrochemically Addressed Cross-links in Polyelectrolyte Multilayers: Cyclic Duravoltammetry. Langmuir. 2011; 27:9418–9424. [PubMed: 21718024]
16. Müller M, Rieser T, Köthe M, Kessler B, Brissova M, Lunkwitz K. Deposition and Bioadhesion Properties of Polymer Multilayers. An In-situ-ATR-FTIR-study. Macromol Symp. 1999; 145:149–159.
17. Ladam G, Gergely C, Senger B, Decher G, Voegel JC, Schaaf P, Cuisinier FJG. Protein Interactions with Polyelectrolyte Multilayers: Interactions between Human Serum Albumin and Polystyrene Sulfonate/Polyallylamine Multilayers. Biomacromolecules. 2000; 1:674–687. [PubMed: 11710198]
18. Ladam G, Schaaf P, Cuisinier FJG, Decher G, Voegel JC. Protein Adsorption onto Auto-Assembled Polyelectrolyte Films. Langmuir. 2001; 17:878–882.
19. Salloum DS, Olenych SG, Keller TCS, Schlenoff JB. Vascular Smooth Muscle Cells on Polyelectrolyte Multilayers: Hydrophobicity-Directed Adhesion and Growth. Biomacromolecules. 2005; 6:161–167. [PubMed: 15638516]
20. Izumrudov VA, Kharlampieva E, Sukhishvili SA. Multilayers of a Globular Protein and a Weak Polyacid: Role of Polyacid Ionization in Growth and Decomposition in Salt Solutions. Biomacromolecules. 2005; 6:1782–1788. [PubMed: 15877405]

21. Müller M, Torger B, Kessler B. In situ ATR-FTIR Spectroscopy on the Deposition and Protein Interaction of Polycation/Alginate Multilayers. Adv Biomater. 2010:B676–B683.
22. Richert L, Boulmedais F, Lavalle P, Mutterer J, Ferreux E, Decher G, Schaaf P, Voegel JC, Picart C. Improvement of Stability and Cell Adhesion Properties of Polyelectrolyte Multilayer Films by Chemical Cross-linking. Biomacromolecules. 2004; 5:284–294. [PubMed: 15002986]
23. Semenov OV, Malek A, Bittermann AG, Vörös J, Zisch AH. Engineered Polyelectrolyte Multilayer Substrates for Adhesion, Proliferation, and Differentiation of Human Mesenchymal Stem Cells. Tissue Eng, Part A. 2009; 15:2977–2990. [PubMed: 19320572]
24. Mehrotra S, Hunley SC, Pawelec KM, Zhang L, Lee I, Baek S, Chan C. Cell Adhesive Behavior on Thin Polyelectrolyte Multilayers: Cells Attempt to Achieve Homeostasis of Its Adhesion Energy. Langmuir. 2010; 26:12794–12802. [PubMed: 20604583]
25. Picart C, Lavalle P, Hubert P, Cuisinier FJG, Decher G, Schaaf P, Voegel JC. Buildup Mechanism for Poly(L-lysine)/Hyaluronic Acid Films onto a Solid Surface. Langmuir. 2001; 17:7414–7424.
26. Salomäki M, Loikas K, Kankare J. Effect of Polyelectrolyte Multilayers on the Response of a Quartz Crystal Microbalance. Anal Chem. 2003; 75:5895–5904. [PubMed: 14588031]
27. Gao C, Leporatti S, Moya S, Donath E, Möhwald H. Stability and Mechanical Properties of Polyelectrolyte Capsules Obtained by Stepwise Assembly of Poly(styrenesulfonate sodium salt) and Poly(diallyldimethyl ammonium) Chloride onto Melamine Resin Particles. Langmuir. 2001; 17:3491–3495.
28. Vinogradova OI, Andrienko D, Lulevich VV, Nordschild S, Sukhorukov GB. Young's Modulus of Polyelectrolyte Multilayers from Microcapsule Swelling. Macromolecules. 2004; 37:1113–1117.
29. Nolte AJ, Rubner MF, Cohen RE. Determining the Young's Modulus of Polyelectrolyte Multilayer Films via Stress-Induced Mechanical Buckling Instabilities. Macromolecules. 2005; 38:5367–5370.
30. Domke J, Radmacher M. Measuring the Elastic Properties of Thin Polymer Films with the Atomic Force Microscope. Langmuir. 1998; 14:3320–3325.
31. Cameron AR, Frith JE, Cooper-White JJ. The Influence of Substrate Creep on Mesenchymal Stem Cell Behaviour and Phenotype. Biomaterials. 2011; 32:5979–5993. [PubMed: 21621838]
32. Schwarz B, Schönhoff M. Surface Potential Driven Swelling of Polyelectrolyte Multilayers. Langmuir. 2002; 18:2964–2966.
33. Adusumilli M, Bruening ML. Variation of Ion-Exchange Capacity, ζ Potential, and Ion-Transport Selectivities with the Number of Layers in a Multilayer Polyelectrolyte Film. Langmuir. 2009; 25:7478–7485. [PubMed: 19563229]
34. Chen W, McCarthy TJ. Layer-by-Layer Deposition: A Tool for Polymer Surface Modification. Macromolecules. 1997; 30:78–86.
35. Yoo D, Shiratori SS, Rubner MF. Controlling Bilayer Composition and Surface Wettability of Sequentially Adsorbed Multilayers of Weak Polyelectrolytes. Macromolecules. 1998; 31:4309–4318.
36. Wong JE, Rehfeldt F, Haenni P, Tanaka M, Klitzing Rv. Swelling Behavior of Polyelectrolyte Multilayers in Saturated Water Vapor. Macromolecules. 2004; 37:7285–7289.
37. Smith RN, Reven L, Barrett CJ. 13C Solid-State NMR Study of Polyelectrolyte Multilayers. Macromolecules. 2003; 36:1876–1881.
38. McCormick M, Smith RN, Graf R, Barrett CJ, Reven L, Spiess HW. NMR Studies of the Effect of Adsorbed Water on Polyelectrolyte Multilayer Films in the Solid State. Macromolecules. 2003; 36:3616–3625.
39. Smith RN, McCormick M, Barrett CJ, Reven L, Spiess HW. NMR Studies of PAH/PSS Polyelectrolyte Multilayers Adsorbed onto Silica. Macromolecules. 2004; 37:4830–4838.
40. Schönhoff M, Ball V, Bausch AR, Dejugnat C, Delorme N, Glinel K, Von Klitzing R, Steitz R. Hydration and Internal Properties of Polyelectrolyte Multilayers. Colloids Surf, A. 2007; 303:14–29.
41. Miller MD, Bruening ML. Correlation of the Swelling and Permeability of Polyelectrolyte Multilayer Films. Chem Mater. 2005; 17:5375–5381.
42. Iturri Ramos JJ, Stahl S, Richter RP, Moya SE. Water Content and Buildup of Poly(diallyldimethylammonium chloride)/Poly(sodium 4-styrenesulfonate) and Poly(allylamine

hydrochloride)/Poly(sodium 4-styrenesulfonate) Polyelectrolyte Multilayers Studied by an in Situ Combination of a Quartz Crystal Microbalance with Dissipation Monitoring and Spectroscopic Ellipsometry. Macromolecules. 2010; 43:9063–9070.

43. Schlenoff JB, Rmaile AH, Bucur CB. Hydration Contributions to Association in Polyelectrolyte Multilayers and Complexes: Visualizing Hydrophobicity. J Am Chem Soc. 2008; 130:13589–13597. [PubMed: 18798621]
44. Mueller R, Koehler K, Weinkamer R, Sukhorukov G, Fery A. Melting of PDADMAC/PSS Capsules Investigated with AFM Force Spectroscopy. Macromolecules. 2005; 38:9766–9771.
45. Francius G, Hemmerlé J, Ball V, Lavalle P, Picart C, Voegel JC, Schaaf P, Senger B. Stiffening of Soft Polyelectrolyte Architectures by Multilayer Capping Evidenced by Viscoelastic Analysis of AFM Indentation Measurements. J Phys Chem C. 2007; 111:8299–8306.
46. Lu H, Huang G, Wang B, Mamedov A, Gupta S. Characterization of the Linear Viscoelastic Behavior of Single-Wall Carbon Nanotube/Polyelectrolyte Multilayer Nanocomposite Film Using Nanoindentation. Thin Solid Films. 2006; 500:197–202.
47. Shiratori SS, Rubner MF. pH-Dependent Thickness Behavior of Sequentially Adsorbed Layers of Weak Polyelectrolytes. Macromolecules. 2000; 33:4213–4219.
48. McAloney RA, Sinyor M, Dudnik V, Goh MC. Atomic Force Microscopy Studies of Salt Effects on Polyelectrolyte Multilayer Film Morphology. Langmuir. 2001; 17:6655–6663.
49. Schoeler B, Poptoshev E, Caruso F. Growth of Multilayer Films of Fixed and Variable Charge Density Polyelectrolytes: Effect of Mutual Charge and Secondary Interactions. Macromolecules. 2003; 36:5258–5264.
50. Poptoshev E, Schoeler B, Caruso F. Influence of Solvent Quality on the Growth of Polyelectrolyte Multilayers. Langmuir. 2004; 20:829–834. [PubMed: 15773111]
51. Garza JM, Schaaf P, Muller S, Ball V, Stoltz JF, Voegel JC, Lavalle P. Multicompartment Films Made of Alternate Plyelectrolyte Multilayers of Exponential and Linear Growth. Langmuir. 2004; 20:7298–7302. [PubMed: 15301518]
52. Cornelsen M, Helm CA, Block S. Destabilization of Polyelectrolyte Multilayers Formed at Different Temperatures and Ion Concentrations. Macromolecules. 2010; 43:4300–4309.
53. Mendelsohn JD, Barrett CJ, Chan VV, Pal AJ, Mayes AM, Rubner MF. Fabrication of Microporous Thin Films from Polyelectrolyte Multilayers. Langmuir. 2000; 16:5017–5023.
54. Fery A, Schoeler B, Cassagneau T, Caruso F. Nanoporous Thin Films Formed by Salt-Induced Structural Changes in Multilayers of Poly(acrylic acid) and Poly(allylamine). Langmuir. 2001; 17:3779–3783.
55. Schlenoff JB, Dubas ST. Mechanism of Polyelectrolyte Multilayer Growth: Charge Overcompensation and Distribution. Macromolecules. 2001; 34:592–598.
56. Gao L, McCarthy TJ. Wetting 101°. Langmuir. 2009; 25:14105–14115. [PubMed: 19627073]
57. Buck ME, Schwartz SC, Lynn DM. Superhydrophobic Thin Films Fabricated by Reactive Layer-by-Layer Assembly of Azlactone-Functionalized Polymers. Chem Mater. 2010; 22:6319–6327. [PubMed: 21151704]
58. Park JH, Schwartz Z, Olivares-Navarrete R, Boyan BD, Tannenbaum R. Enhancement of Surface Wettability via the Modification of Microtextured Titanium Implant Surfaces with Polyelectrolytes. Langmuir. 2011; 27:5976–5985. [PubMed: 21513319]
59. Salloum DS, Schlenoff JB. Protein Adsorption Modalities on Polyelectrolyte Multilayers. Biomacromolecules. 2004; 5:1089–1096. [PubMed: 15132703]

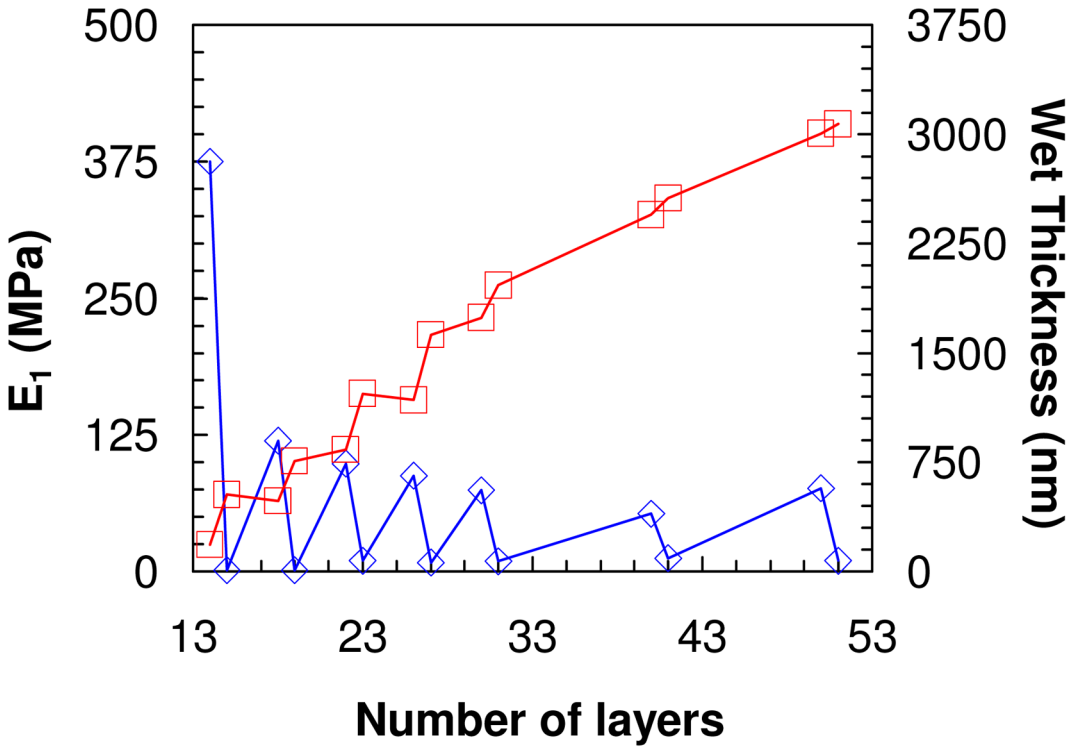

Figure 1.

(□) Wet thickness of PDADMA/PSS multilayer as a function of number of layers. (◊) apparent surface Young's modulus obtained by force curve measurement taken at layer number 14, 15, 18, 19, 22, 23, 26, 27, 30, 31, 40, 41, 50 and 51. All measurements were performed *in situ* in 10 mM NaCl. An odd number of layers represents a PEMU capped with PDADMA and even corresponds to PSS-terminated film.

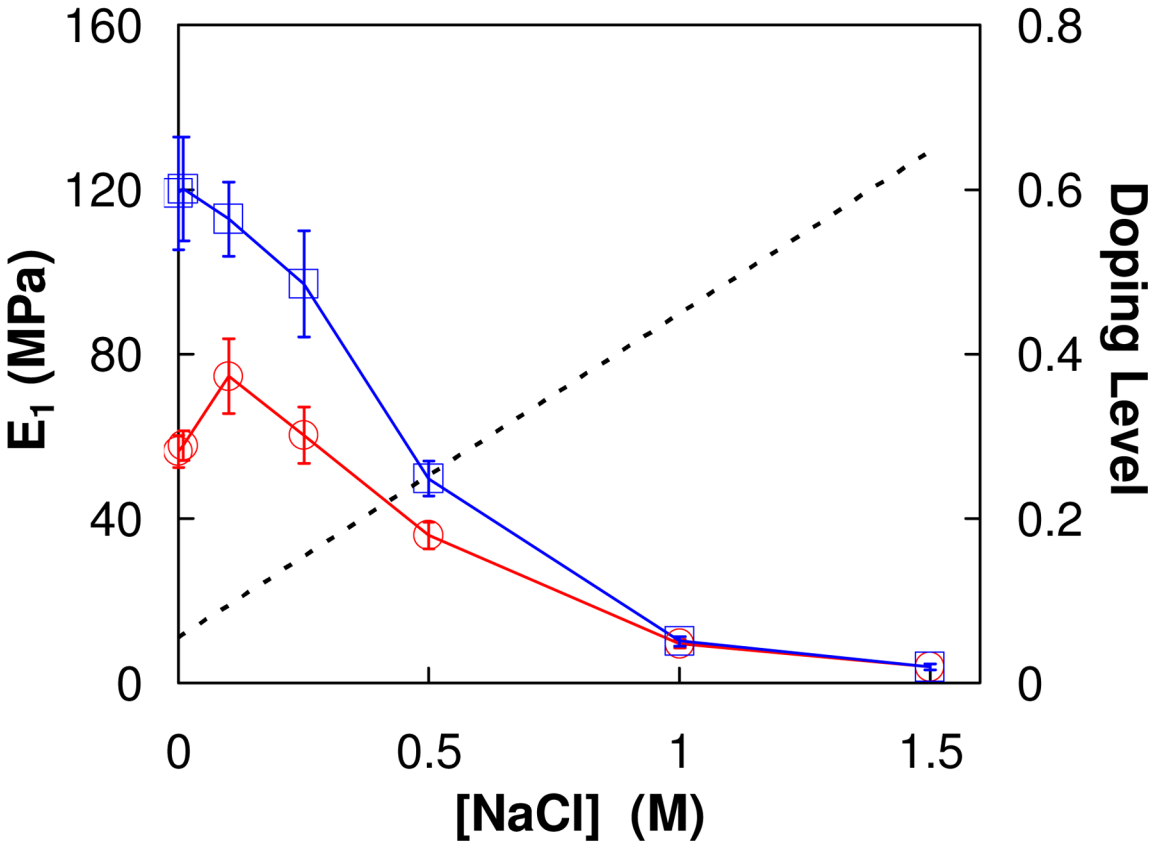

Figure 2.
Apparent Young's modulus of a $(PDADMA/PSS)_{15}$ multilayer prepared at 1 M NaCl with increasing [NaCl] (○); then decreasing [NaCl] (□). The tip velocity was 1μm/s. The dotted line represents the doping level as a function of [NaCl].

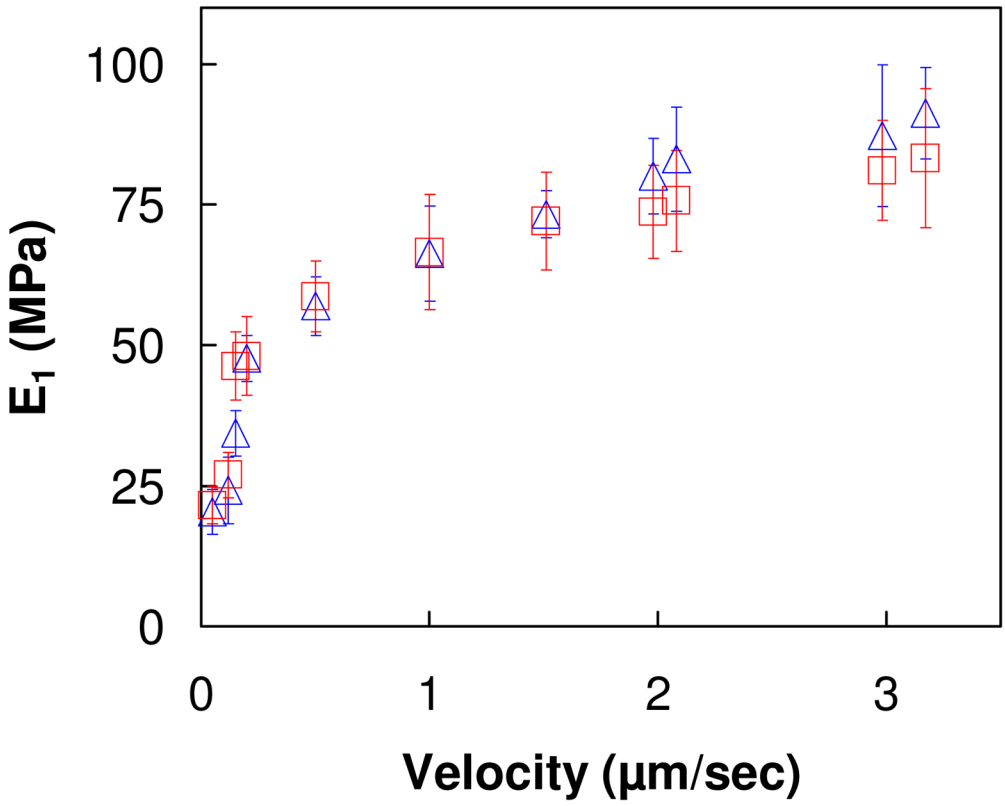

Figure 3.

Apparent Young's modulus of $(PDADMA/PSS)_{15}$ multilayer surfaces, one un-annealed (□), the other annealed in 1 M NaCl (△), at different indentation velocities. The salt concentration of the polyelectrolyte solution was 1 M NaCl during build up and 10 mM for these *in situ* indentations, which probe the top 50 nm of the PEMU. The indentation velocity varied from 50 nm/sec to 3.15 μm/sec.

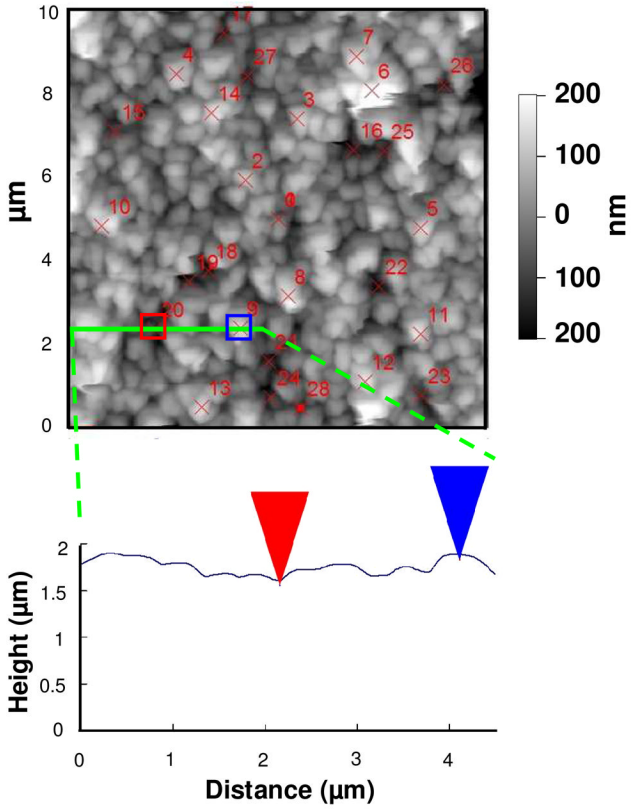

Figure 4.

AFM image of a $(PDADMA/PSS)_{16}$ multilayer, was taken in 10 mM NaCl. The red crosses represent positions where force curves were taken. 14 force curves on the hills (bright grey spots) gave an average modulus of 47 MPa, and 14 force curves in the valleys (dark grey area) resulted in an average modulus of 49 MPa. The 4 µm-long solid line was drawn through point 20 (valley) and 9 (hill) and the contour shown in the height *vs*. distance graph. The thickness of the PEMU was measured at a scratch edge.

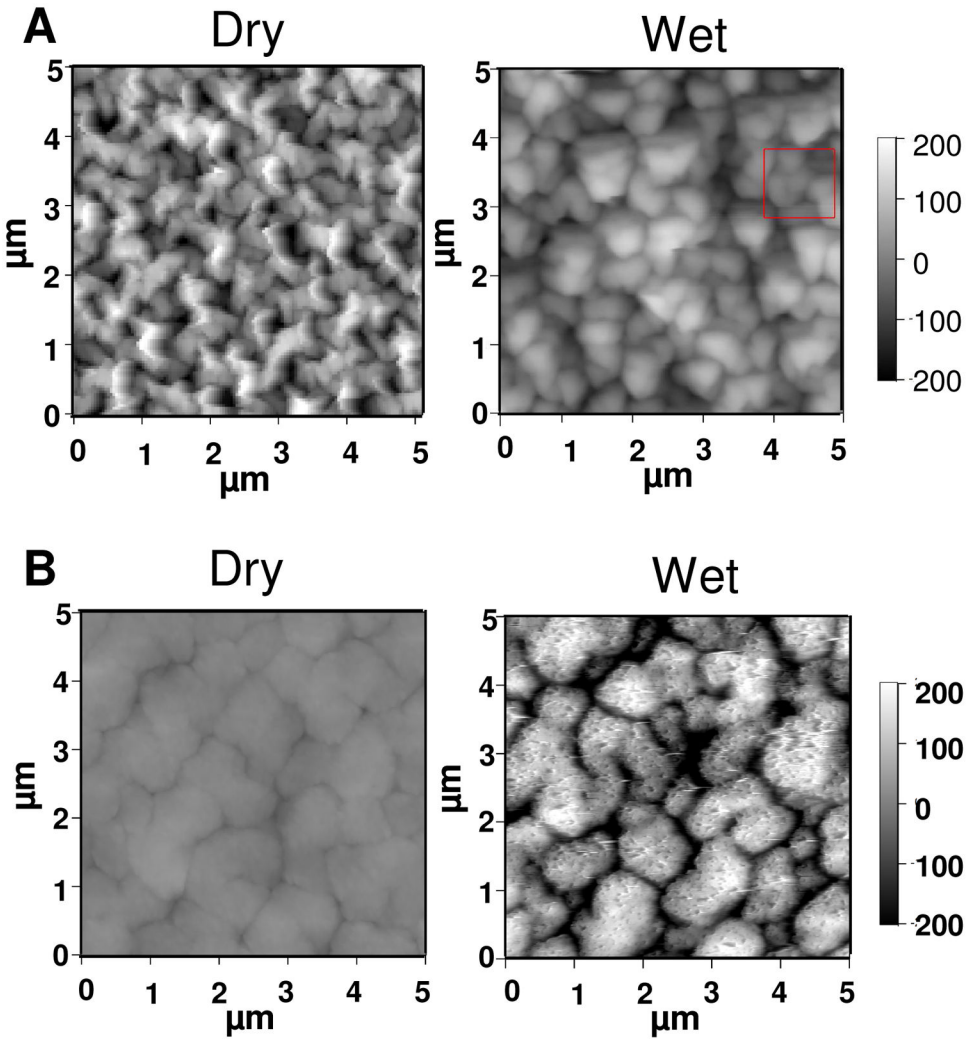

Figure 5.

A and B are images of dry and wet $(PDADMA/PSS)_{15}$ and $(PDADMA/PSS)_{15}PDADMA$ multilayer, respectively. The images of wet PEMU were taken while the multilayer was immersed in 10 mM NaCl. For the PSS-ending film the surface roughness was 66 nm and 70 nm for dry and wet respectively, and that of PDADMA ending film was 16 nm and 106 nm for dry and wet respectively.

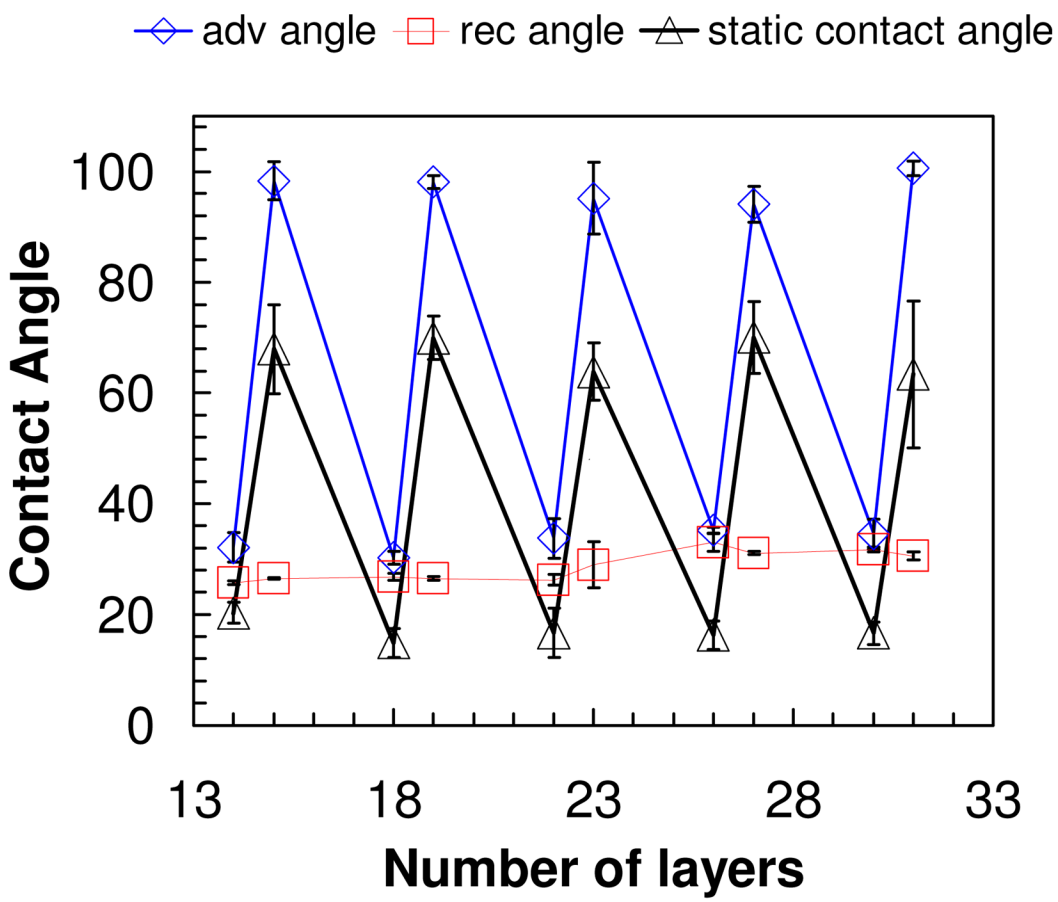

Figure 6.
(◊), (Δ), (□) the advancing, static and receding contact angle of PDADMA/PSS multilayer as a function layer number. Odd layers are PDADMA and even layers PSS.

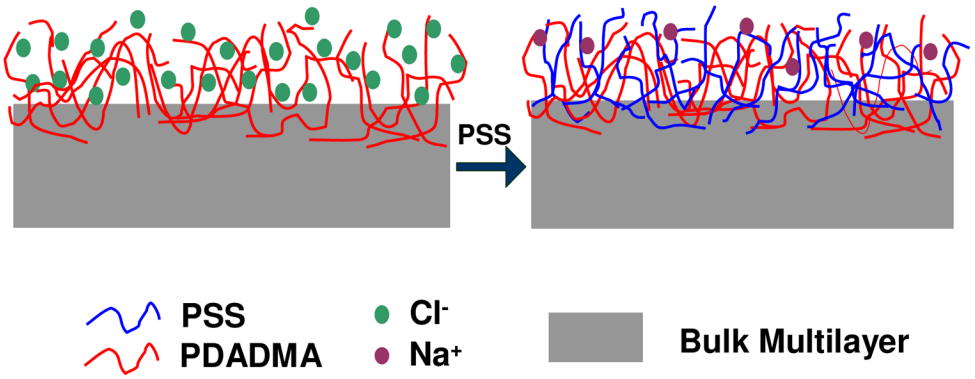

Scheme 1.
Multilayer ending in PDADMA (left) showing the presence of extrinsic sites; the addition of PSS converts almost all extrinsic sites into intrinsic ones.